Surface heat flow in Western Anatolia (Turkey) and implications to the thermal structure of the Gediz Graben

Elif BALKAN-PAZVANTOĞLU[1],* , Kamil ERKAN[2] , Müjgan ŞALK[1] , Bülent Oktay AKKOYUNLU[3] , Mete TAYANÇ[2]

[1]Department of Geophysical Engineering, Dokuz Eylül University, İzmir, Turkey,
[2]Department of Environmental Engineering, Marmara University, İstanbul, Turkey,
[3]Department of Physics, Marmara University, İstanbul, Turkey

Abstract: Knowledge of heat flow density on the Earth's surface and subsurface temperature distribution is essential for the interpretation of several processes in the crust such as for the evaluation of the geothermal potential of a region. With this study, we investigate the conductive heat flow distribution in western Anatolia to understand the thermal state and its relationship to regional tectonics in the region. The new heat flow data are collected and combined with previously published data to obtain the new heat flow map of western Anatolia. Analysis of data sets after appropriate corrections yields a better picture of the regional distribution of heat flow within the region. Generally, high values are observed around the grabens of Menderes Massif due to the intense tectonic activity. We also present the 2D steady-state thermal model of Gediz. The modeled temperatures are validated by temperature measurements from two deep wells. Numerical simulation results show that the dominant heat transfer mechanism in Gediz graben can be explained by conduction. Temperature distribution in the deep subsurface of the graben is controlled by both thickness distribution and thermal properties of the different stratigraphic sections. Thermal conductivity contrast between different stratigraphic sections causes anomalously elevated heat flow values at the edges of the graben. The comprehensive results of this study will bring a new perspective to geothermal studies in particular Enhanced Geothermal Systems (EGS) resource estimations in Gediz graben.

Key words: Heat flow, geothermal gradient, thermal model, western Anatolia, Gediz graben, geothermal energy

1. Introduction

Knowledge of the heat flow density on the Earth's surface allows us to predict the thermal conditions of the deeper parts, which are not accessible for temperature measurements. Lithology, surface topography, groundwater (cold or thermal) circulation, young volcanism, variable radiogenic heat generation content, mantle heat flow, sedimentation effect at basins, basement structure, and tectonic activity are the predominant factors that can affect the surface heat flow (Lee and Uyeda, 1965; Pollack and Chapman, 1977; Cermak and Rybach, 1979; Jaupart and Labrosse, 2007). To find out their relative contribution to surface heat flow density and to characterize these processes are, therefore, of special interest for recent studies. This study presents the results of the new heat flow data collected from western Anatolia, which is one of the tectonically active continental regions in the world. Due to its intense plate tectonic activity the study area has known for its high heat flow values in the limited number of previous conventional heat flow studies (Tezcan and

Turgay, 1991; Pfister et al., 1998; Erkan, 2015). It was suggested that significant extension is responsible for the thermal structure of the region (Çağlar, 1961; Demirel and Şentürk, 1996; Karakuş, 2013; Roche et al., 2019). Western Anatolia stands with high heat values in the Turkey heat flow map of Tezcan and Turgay (1991), which was based on bottom-hole temperature data from deep wells and a constant thermal conductivity assumption. Pfister et al. (1998) published geothermal gradients from equilibrium wells and thermal conductivity measurements from outcrops for the northwestern part of the region. Erkan (2015) prepared a preliminary heat flow map of western Anatolia using high-resolution equilibrium temperature logs from shallow boreholes and thermal conductivities measured from outcrops or estimated by the lithology of related rocks. The heat flow map outlines areas of high heat flow (85–95 mW m^{-2}) in the coastal parts of the region (peninsular areas of Çanakkale and İzmir provinces) and the central part of Menderes Massif (>100 mW m^{-2} in Kula volcanic region) but moderate heat flow values (55–70 mW

* Correspondence: elif.balkan@deu.edu.tr

m^{-2}) in some of the interior parts including central part of Balıkesir and the west of Manisa provinces. Menderes Massif province hosts the highest enthalpy geothermal systems of Turkey and the bottom-hole temperatures (BHTs) in geothermal wells reach up the 287 °C in Gediz graben and 247 °C in Büyük Menderes graben (Baba, 2012; Karakuş and Şimşek, 2012). These high temperatures were interpreted by the transfer of the heat from the shallow mantle to the surface by the circulation of fluids using the low-angle faults systems. Geophysical studies imply the high potential for development of enhanced geothermal systems (EGS) in the Alaşehir part of the Gediz graben (Burçak, 2012, 2015; Hıdıroğlu and Parlaktuna, 2019). Even though exploration-based studies demonstrate that there is a significant geothermal resource base in western Anatolia, conventional heat flow studies have been very limited in the region. The lack of sufficient amount thermal conductivity and the geothermal gradient data are the main reasons for the limited number of heat flow studies in the area.

In this study, the new high-resolution equilibrium temperatures were collected for 30 sites from western Anatolia (Figure 1a). Thermal conductivities were determined from measurements of outcrops of related rock or assigned from literature based on the lithological information. After correcting for effects of the groundwater flow, sedimentation, erosion, and paleoclimatic changes, we reported 21 geothermal gradients and 19 heat flow determinations for the region. Erkan (2015) published geothermal gradients for western Anatolia, but due to the lack of thermal conductivity information, heat flow values were not calculated for 12 of them. In this study, we also included these 12 geothermal gradient data into our data set and calculated heat flow after evaluating thermal conductivity information.

The heat flow map of western Anatolia is updated using the new and the previously published data (Pfister et al., 1998; Erkan, 2015) (Figure 1a) and compared with the results of earlier studies. In the light of new heat flow data, we develop 2-D conductive thermal model using the seismic and well data for the Gediz graben. Calculated model approaches compared against measured temperatures observed from two deep wells. Obtained temperature distribution provides geothermal gradient information for the region. This data may be the initial step for replying to the question of whether there is enough heat for possible EGS resources to existing in the Gediz graben.

2. Study area and geological settings
Western Anatolia has a seismically active crust with an extensional regime and subduction-related volcanism. Interaction within the Eurasia, Arabia, and Africa plates and Aegean-Cyprian subduction controls the large deformation in the province (Dewey and Şengör, 1979; Şengör et al., 1985; Bozkurt, 2001). Crustal thinning and internal deformation of the Anatolian microplate dominate in the region in the form of approximately north-south oriented extension (Le Pichon et al., 1995). Due to the extensional regime, the upper part of the crust has been broken by faults; thus, E-W trending graben systems prevail in the region (Yılmaz, 2000). Gediz and Büyük Menderes grabens are the largest grabens developed within the Menderes Massif Province. Both thicknesses of sedimentary sections and displacement on the bounding faults are greater compared with the other basins (Işık and Tekeli, 2001; Hakyemez et al., 1999).

Gediz graben extends more than 150 km along the Gediz River and has approximately 40 km width at its western end, and becomes narrow eastward until it dies out (Figure 1a and b). Gediz evolved as an asymmetric graben bounded by normal faults dominantly active at the southern margin through the entire Miocene, developing into a graben as a result of post-Miocene faulting of the northern margin (Emre, 1996; Yılmaz et al., 2000; Sözbilir, 2002; Ciftçi and Bozkurt, 2009a; Gülmez et al., 2019). The southern master graben-bounding fault (MGBF) plays a critical role in its deformation and deposition. Depositional geometry of Gediz graben was provided Çiftçi and Bozkurt (2009a and 2009b), using 270 km length 2D seismic reflection data interpreted with logs from three boreholes (Figure 2a, b, and c) and outcrops. Seismic reflection profile S-12 (Figure 2b) shows the geometry and bonding structure of the Gediz graben and emphasizes its asymmetric nature. Three main seismic stratigraphic units (SSU) overlying metamorphic basement were identified by Çifçti and Bozkurt (2009a) on the seismic reflection profile. Metamorphic rocks of the Menderes Massif which are composed of mainly schists, marbles, quartzites, and phyllites represent the basement unit in Gediz graben (Işık and Tekeli, 2001). The estimated thickness of the graben fills ranges between 1.5–4 km (Paton, 1992; Gürer et al., 2002; Sarı and Şalk, 2006; Özyalın et al., 2012). The Alaşehir formation (SSU–I) unit generally consists of shale and conglomerates (Figure 2b). The Alaşehir formation is overlain by the Çaltılık formation (SSU–II), which contains limestones. Gediz, Kaltepe and Bintepeler formations (SSU–IIIa) are located on the Çaltılık formation. All of these are covered by the Quaternary alluvium of SSU–IIIb (Çiftçi and Bozkurt, 2010).

3. Data collection
To calculate heat flow on land, temperature as a function of depth (T-D) in a borehole is required to derive a geothermal gradient together with the thermal conductivity of the related geologic unit (Lowrie, 2007). The accuracy of the heat flow measurements depends on the precision of temperature data and thermal conductivity measurements performed in the laboratory.
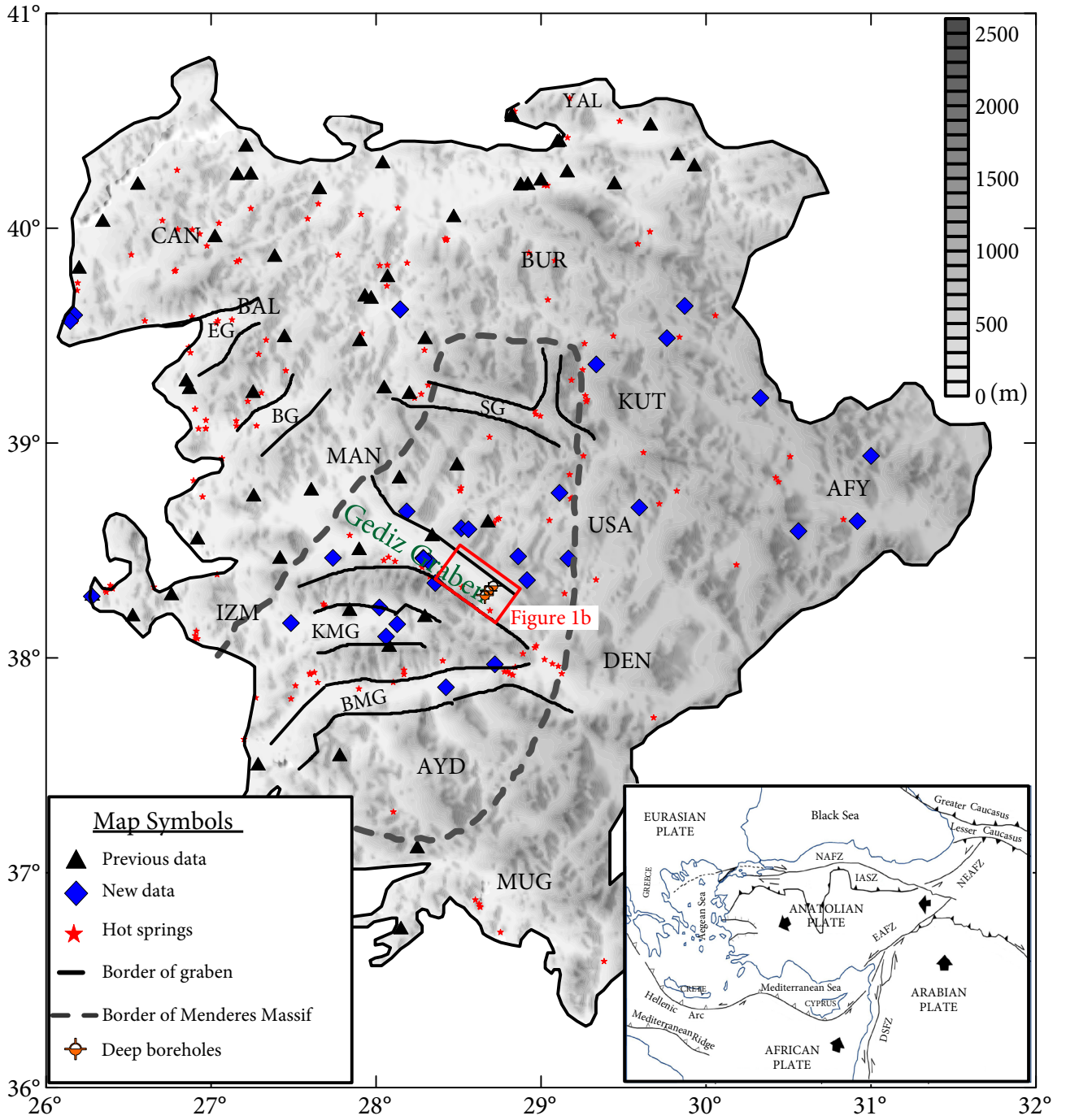
Figure 1. a) Study area with data locations. Previously published data are displayed as black triangles and newly collected data for this study are as blue diamonds. Red stars represent the hot spring and the black dashed line shows the boundary of Menderes Massif. Elevations are in meters. BMG: Büyük Menderes Graben; KMG: Küçük Menderes Graben; EG: Edremit Graben; BG: Bakırçay Graben; SG: Simav Graben; AYD:Aydın; AFY: Afyon; BAL: Balıkesir; BUR: Bursa; CAN: Çanakkale; DEN:Denizli; IZM: İzmir; KUT: Kütahya; MAN: Manisa; MUG:Muğla; USA:Uşak.

The new data set reported in this study consist of new measurements (both T-D and thermal conductivity) and previously published geothermal gradients (İlkışık et al., 1996, İlkışık et al., 1996b, Erkan, 2015) whose heat flow values were not calculated due to the lack of thermal conductivity information. Thermal conductivity information related to 12 sites are achieved, and they are included in our data set after calculated heat flow values.
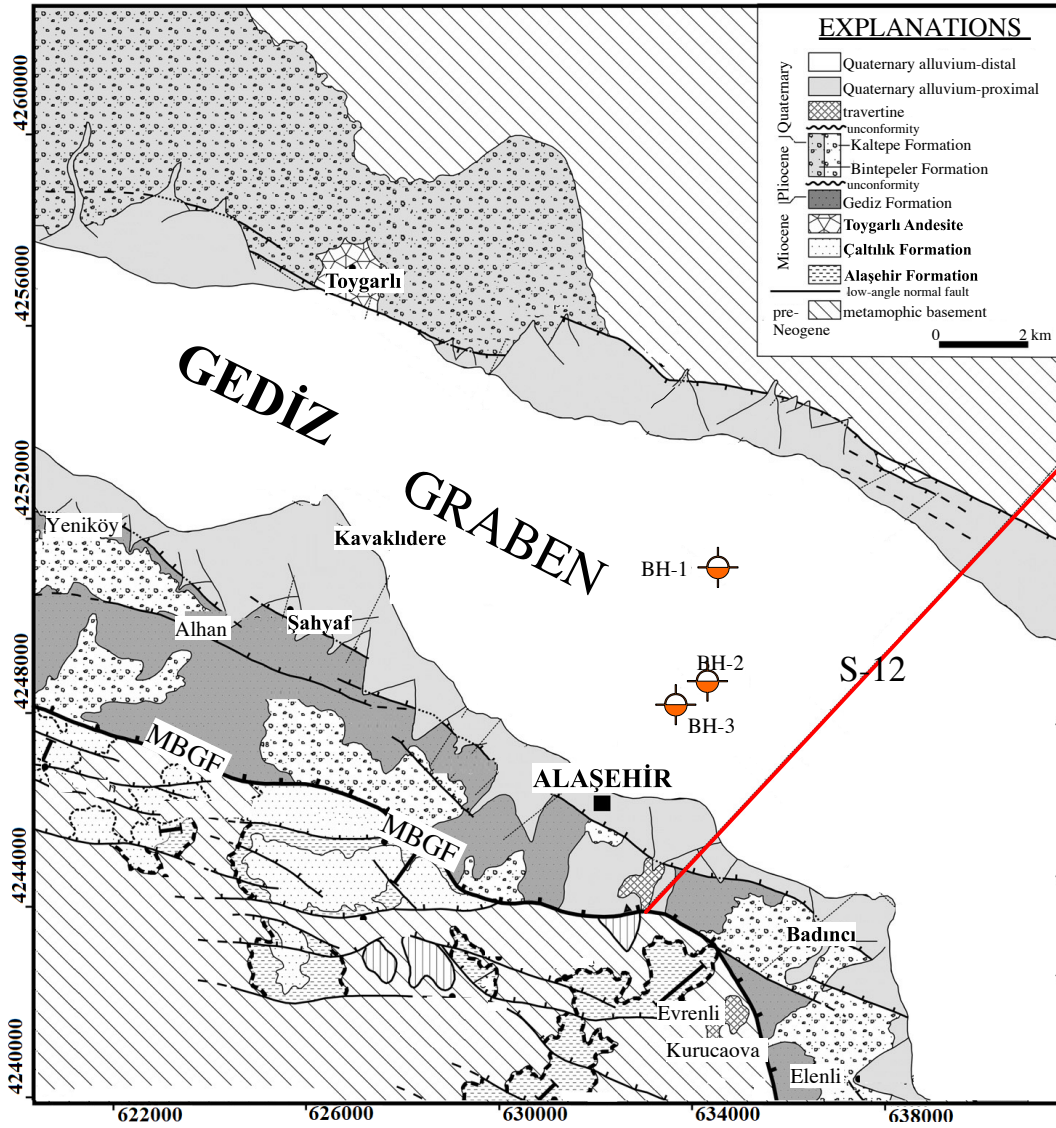
Figure 1.b) Geological map of the Gediz graben around Alaşehir showing major structures, geological units, location of the boreholes and seismic profile (S-12) (Çiftçi and Bozkurt, 2009a). MGBF: master graben bounding fault; BH: borehole.

The second data set consisting of new high-resolution temperature-depth (T-D) data set are collected from Aydın, Balıkesir, Çanakkale, İzmir, Kütahya, Uşak, and Manisa provinces (Figure 1). Field measurements were performed between the years of 2013 and 2016 temperature-depth data from 30 water wells, at a maximum depth not exceeding 300 m. The wells were partly provided by the State Hydrological Works (DSI) regional directorates and partly by local private drilling companies. The wells were drilled for water supply or monitoring groundwater. Measurements were conducted in unused (not producing) or abandoned wells. Location, depth, static water level, lithologic information, etc. were obtained from the personnel of the state offices or the

drillers. T-D measurements are recorded below the water table using a custom-designed thermistor probe four-wire portable tool in the acquisition of the data with the 1–5 m sampling interval.

Thermal conductivity measurements were done on the rock samples collected from surface outcrops in the vicinity of certain boreholes using the QTM-500 (Quick Thermal conductivity Meter) in the laboratory of Dokuz Eylül University. The QTM-500 device is based on the ASTM C 1113-90 hot wire method (Healy et al., 1976). It is an effective and reliable technique for measuring thermal conductivity (Grubbe et al., 1983; Sass et al 1984). QTM-500 is widely used in thermal conductivity determinations of rocks due to the advantage of rapid sampling time
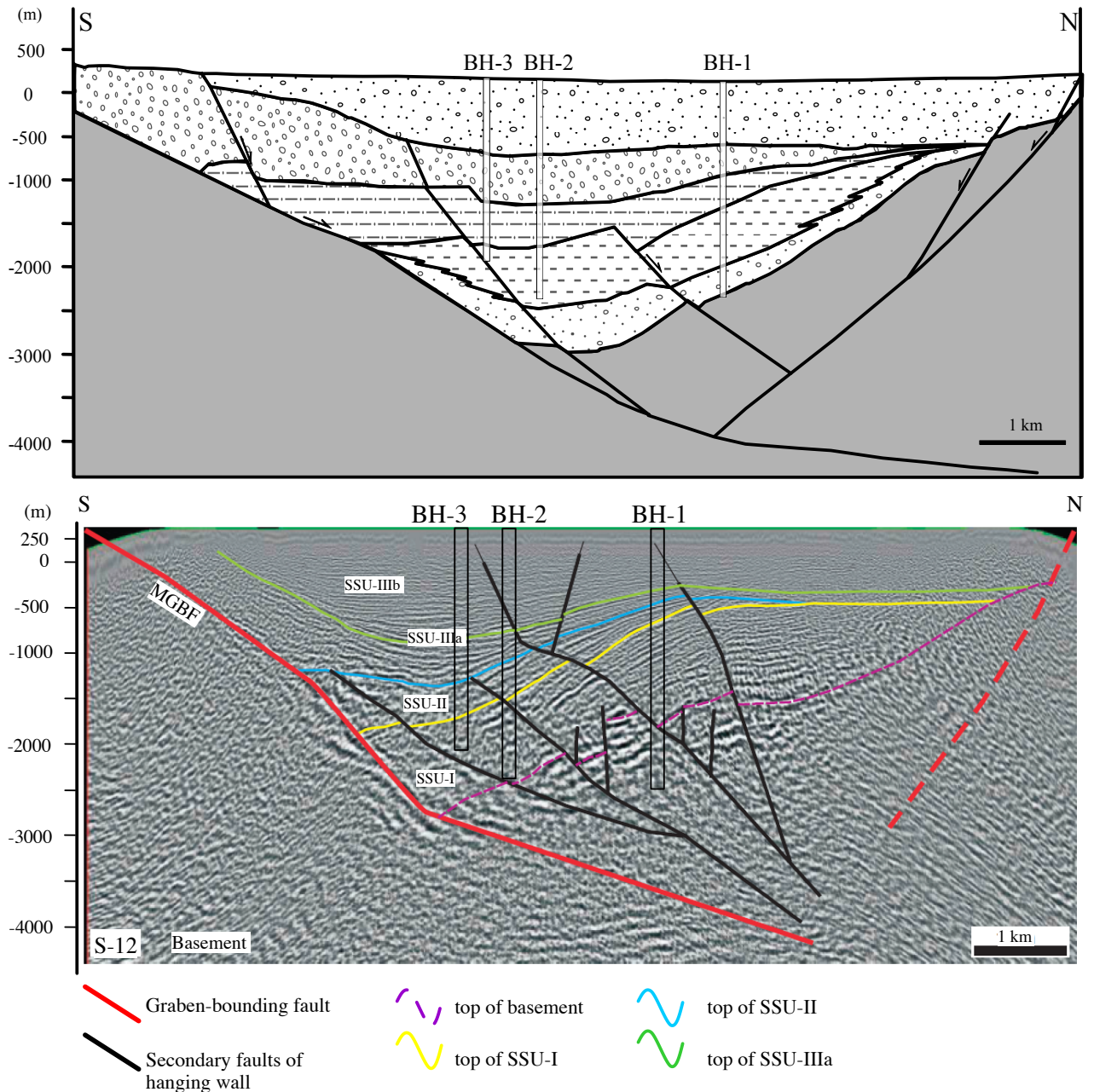
Figure 2. a) Geological cross-section of Gediz graben. b) Seismic reflection profile showing the depositional geometry and the correlation of the seismic stratigraphic units (SSU) (Çiftçi&Bozkurt, 2010) (See Figure 1b for the location), A summary section of the deep boreholes drilled in Gediz graben (Çiftçi & Bozkurt, 2009a).

(Thienprasert and Raksaskulwong 1984; Demirboğa 2003; Çanakci et al 2007; Bellani and Gherardi, 2019). All thermal conductivity measurements are done on rock samples under ambient temperature and pressure after saturated with water minimum 48 h.

4. Data analysis

Recorded T-D measurements within the boreholes may be distributed by hydrogeological effects, climatic changes,

and topographic contrasts around mountainous terrains. To evaluate reliable heat flow values, the effects of these factors must be corrected. Related corrections were applied to our T-D data set, if necessary.

4.1. T-D data quality classifications

Hydrogeological effects under the earth's surface, climatic changes, and topographic differences around the mountainous provinces cause some perturbations on T-D measurements. The influence of these factors must be

removed from the T-D data to evaluate accurate heat flow values.

In this study, generally, T-D data are recorded in the boreholes drilled for hydrogeological purposes; thus, they were disturbed by the local hydrological effects. In order to eliminate these effects, we applied the method of Erkan (2015) for quality classification given in Table 1. According to Erkan (2015), class A and B data represent the solution of 1-D heat transfer along a borehole (Jaeger, 1965). This kind of data consists of a linearly increasing temperature with depth and should extrapolate to the mean annual ground surface temperature (GST) at the measurement point. Vertical fluid flow in some sections of a borehole (intra-borehole fluid flow) results in a partly disturbed T-D curve. Such kinds of data are classified as class C. If water movement affects the large part of the T-D curve, or the borehole is too shallow (< 50 m), it is rated as class D. If the T-D curves are completely under the influence of groundwater movement, they are not used for heat flow determination and rated class X. Some sites show the effect of local geothermal activity, which shows distinctly higher temperatures. These types of data are rated class G and are also not suitable for conductive heat flow determinations (Erkan, 2015).

In this study, out of the 30 new sites, nine borehole sites fall into class X and they were not taken into consideration in geothermal gradient calculations. Four sites are found to be under geothermal activity (G). The remaining 17 sites are suitable for the conductive thermal regime from Class A to Class D. Class A and B holes are the most reliable sites where the entire T-D data show conductive (linear) behavior. Class C holes show intra-borehole fluid flow (IBF) activity in some sections. Class D holes are the least reliable sites with highly disturbed by the IBF activity.

4.2. Topographic correction

The steep topography differences near the T-D measurement point exhibit larger variation in subsurface temperature distribution under the mountainous regions (Beardsmore and Cull, 2001). Lees (1910) suggested a correction to eliminate the disturbance in the geothermal

field beneath an idealized mountain range. Uncorrected data yields us significant errors in geothermal gradient determinations. In this study, Lees' (1910) correction was applied for H.embelli, Kaymakçı, and Osmancık boreholes where steep topographic changes were observed near the measuring point and the corrected geothermal gradients (cG) are listed in (Table 2).

5. Results

5.1. Temperature-depth curves

Classes A/B/C/D/G type T-D data located in the same or adjacent provinces are plotted in several graphs in Figure 3. Interpretation of nearby boreholes enables us to compare surface temperatures with their elevations. The elevation of the borehole can be used as a reference for the expected ground surface temperatures in the vicinity of each borehole site. Calculated geothermal gradients for related interval depth are given with other information in Table 2.

Boreholes recorded in Manisa are shown in Figure 3a. Göbekli, Köseali, and Köseali2 wells are rated as G class with elevated geothermal gradients (72 °C km^{-1}, 113 °C km^{-1}, and 104 °C km^{-1}, respectively). Interestingly, lateral cold water movement perturbs the Göbekli curve at shallow depths. The effect of downflow is noticed below the 80 m in H.embelli. Local hydrological effects disturb at the first 100 m in both of Emreköy and Saraçlar wells. In Osmancık, the effect of lateral flow reaches down to 130 m, and this level acts like the apparent surface of the well. Below 130 m, the T-D curve linearly increases with depth. Poyrazköy is an A class T-D curve with a length of 107 m linear conductive section.

T-D curves for İzmir are given in Figure 3b. A strong IBF inferred on Bademli1 well. Below 50m, a downflow disturbed the Bademli1 curve. T-D curve is recorded within the air section through the K.avulcuk well which may explain distortions from linearity. The conductive section is apparent for both Kaymakçı and Çırpı well below the water table. For Altınkum, higher temperatures near the surface (~ at first 50 m) reflect the recent changes

Table 1. Explanation of the data quality classes used in this study (Erkan, 2015).

Class	Criteria	Relative error in Geothermal gradient
A	Greater than 100m conductive (linear) T –D section	5 %
B	Greater than 50m conductive (linear) T –D section	10%
C	Disturbed T –D curve due to intra-borehole fluid activity. Intermittent conductive sections	25%
D	Intense intra-borehole fluid activity; conductive section too shallow	-
G	Dominated regional geothermal activity on T-D curve (Convective wells)	not suitable
X	Dominated groundwater activity on T-D curve	not suitable

Table 2. A/B/C/D/G-type data used in this study, along with gradients (G), corrected gradients (cG) after topographic correction, thermal conductivities (λ), heat flow (Q) values, and their respective errors. Literature thermal conductivities are marked by (L) next to the value and are obtained from Erkan (2015) for Q.Alluvium and from Balkan et al. (2017) for the other rock types.

Name	Lat	Long	Prov.	Class	Meas. Depth	Elevation	Interval	G	(cor) G	σG	λ	σλ	Q	σQ	Lithology
	(°N)	(°E)				(m)			(°C km^{-1})		W m^{-1} K^{-1}		mW m^{-2}		
[a]Ağzıkara	38.59	30.56	AFY	D	110	1284	0–110	36			1.4	0.2	51		Andesite
Alahabalı	38.47	28.86	USA	A	195	734	65–195	34		2	3.2(L)	0.9	107	36	Schist
Altınkum	38.29	26.28	IZM	B	111	25	42–108	37		4	2.3	0.1	85	12	Marl
Babadere1	39.60	26.17	CAN	G	130	78	70–125	100		10	1.0(L)	0.4	102		Claystone
Bademli1	38.10	28.06	IZM	D	78	230	25–74	38			1.5(L)	0.3	87*		Q. Alluvium fan
[a]Balabancı	38.36	28.91	USA	B	92	716	20–50	38		4	1.5(L)	0.3	57	17	Q. Alluvium
Çırpı	38.16	27.48	IZM	D	45	20	0–38	62			1.5(L)	0.3	93		Q. Alluvium
[a]Darıca	39.64	29.87	KUT	B	90	1165	40–78	50		5	0.7	0.2	35	14	Tuff
[a]Derbent	38.94	31.00	AFY	D	176	1238	120–156	32			1.3(L)	0.6	41		Tuff
Emreköy	38.60	28.52	MAN	B	180	687	100–155	21		2	3.1	0.4	64	14	Schist
Göbekli	38.45	28.32	MAN	G	69	144	25–61	72			1.5(L)	0.3	108		Q. Alluvium
[a]Gümüşkol	38.46	29.17	USA	A	230	895	19–108	52		3	1.3	0.2	68	14	Tuff
[a]Gümüşköy	39.49	29.76	KUT	B	156	1037	28–89	35		4	3.5(L)	1.4	120	60	C Limestone
H.embelli	38.35	28.36	MAN	C	200	846	0–80	27	33	8	3.2(L)	0.9	105	56	Schist
İntepe1	40.00	26.32	CAN	C	136	83	0–136	46		12					
K.avulcuk	38.23	28.02	IZM	D	82	147	25–45	36			1.5(L)	0.3	83*		Q. Alluvium fan
[a]Kadıkoy	38.64	30.92	AFY	D	106	979	0–106	49			1.5(L)	0.3	74		Q. Alluvium
[a]Karakuyu	38.77	29.11	USA	D	114	789	0–108	56			2.8	0.2	156		Limestone
[a]Karlık	38.70	29.60	USA	A	120	1066	34–104	42		2	1.5(L)	0.5	64	24	Marl
Kaymakçı	38.16	28.13	IZM	C	110	147	60–93	33	40	10	1.5(L)	0.3	60	27	Q. Alluvium
[a]Köprücek	39.37	29.33	KUT	C	158	1046	100–150	27	28	7	1.3(L)	0.6	36	26	Tuff
Köprücek1	39.58	29.36	KUT	C	61	1087	37–50	44		11					
Köseali	38.47	28.29	MAN	G	116	160	0–116	113		28	1.5(L)	0.3	170	76	Q. Alluvium
Köseali2	38.46	28.29	MAN	G	113	121	80–108	104		26	1.5(L)	0.3	156	70	Q. Alluvium
Nusrat1	39.62	28.15	BAL	B	110	119	65–115	15		2	1.3(L)	0.6	20	11	Tuff
Nusrat2	39.62	28.15	BAL	B	125	120	80–125	13		1	1.3(L)	0.6	17	10	Tuff
[a]Ortakcı	37.97	28.72	AYD	C	112	211	87–108	38		10	3.5	0.2	132	41	Schist
Osmancık	38.47	27.74	MAN	A	294	298	139–284	24	28	1	1.5(L)	0.3	72*	11	Q. Alluvium fan
Pirlibey	37.86	28.42	AYD	D	25	67	10–25	58			1.5(L)	0.3	117*		Q. Alluvium fan
Poyrazköy	38.68	28.19	MAN	A	167	636	60–167	24		1	3.2(L)	0.9	78	26	Schist
Saraçlar	38.60	28.56	MAN	B	165	694	110–160	25		3	1.2	0.1	30	5	Basalt
[a]Tepeköy	39.21	30.33	KUT	D	182	1100	0–182	31			0.9	0.2	28		Tuff
Tuzla1	39.57	26.15	CAN	B	50	11	10–50	49		5	1.5(L)	0.3	73	22	Q. Alluvium

aGeothermal gradient data are taken from Erkan (2015) and heat flow values are calculated in study.
*Heat flow values corrected for sedimentation effect. Prov:Province; Meas. Depth: Measurement Depth; AFY:Afyon; USA:Uşak; IZM:İzmir; CAN-Çanakkale; KUT:Kütahya; MAN:Manisa; BAL:Balıkesir.

in the MAST but the rest of the curve is suitable for conductive geothermal gradient calculation. In Figure 3c, T-D curves from Aydın, Uşak, and Kütahya are plotted on the same panel. Three T-D measurements were conducted in Aydın, but two of them are rated as X class.

Pirlibey has the shallowest T-D data. Here, only a depth of 15 m conductive layer is used for geothermal gradient calculation. High temperatures are recorded at the first 50 m depth of Alahabali, this is interpreted to be a result of long-term change in the mean annual surface temperature
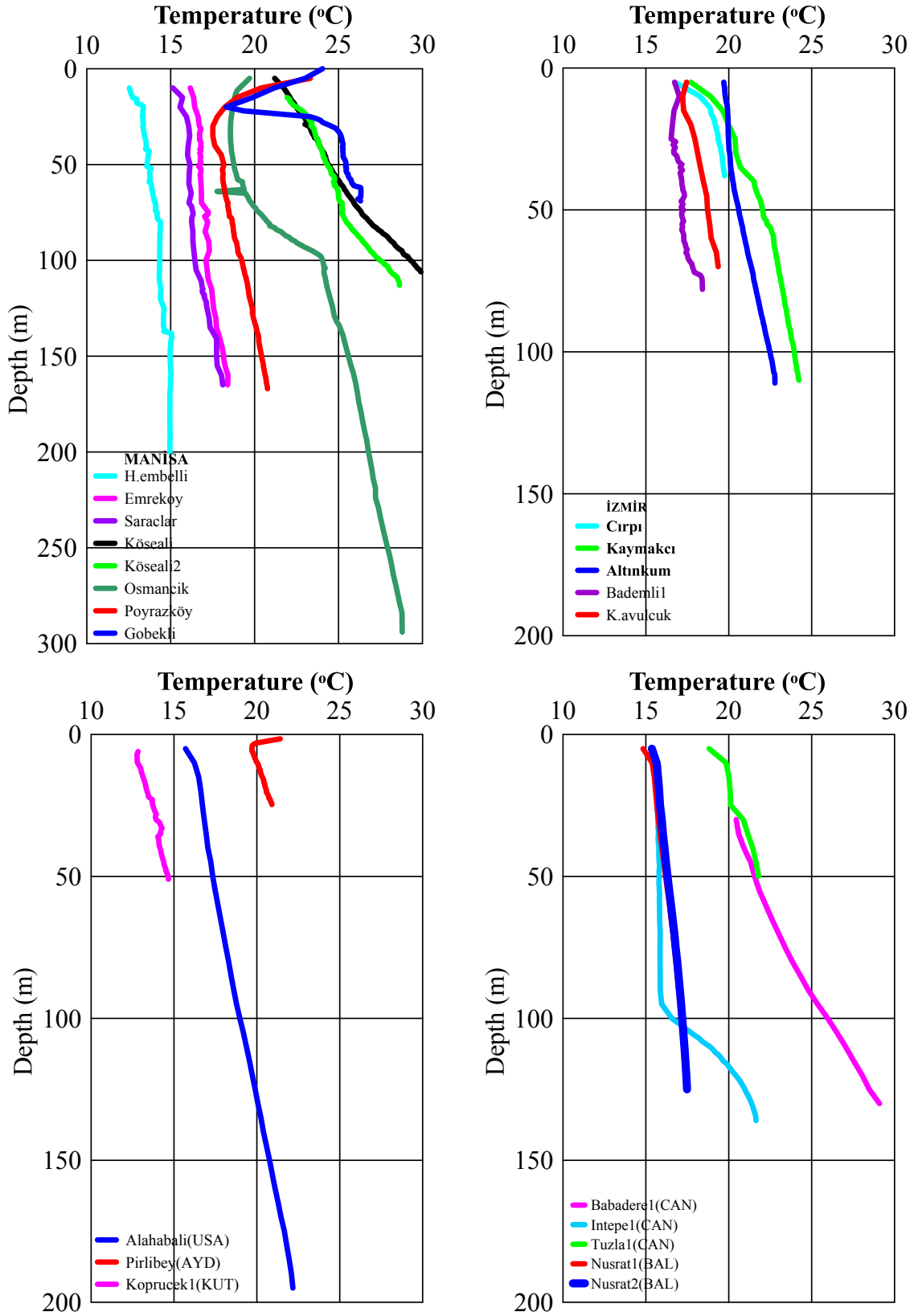
Figure 3. a) Temperature–depth (T–D) curves for Manisa. b) Temperature–depth (T–D) curves for İzmir. c) Temperature–depth (T–D) curves for USA-Uşak, AYD-Aydın, Kut-Kütahya. d) Temperature–depth (T–D) curves for Çanakkale (CAN) and Balıkesir (BAL).

(MAST). The rest of the curve of Alahabali is linearly conductive and classed as A. Köprücek1 in Kütahya shows the conductive behavior, and the effect of IBF is minimal.

T-D curves of Balıkesir are given in Figure 3d. Nusrat1 and Nusrat2 wells are about 500 m apart from each other and are characterized by the conductive thermal regime for almost their entire depths. The projected surface temperatures for them match the MAST of the area.

Four T-D data are recorded in Çanakkale. Babadere1 well is rated as G class with the elevated geothermal gradient. Babadere2 well is logged one day after the drilling process so it is rated as X due to the nonequilibrium conditions. Intepe1 and Tuzla1 wells are suitable for conductive geothermal gradient calculations. Intepe1 well is under the effect of downflow, so the geothermal gradient is calculated using bottom hole temperature and the projected surface temperature. The effect of IBF is minimal on Tuzla1 well (Figure 3d).

5.2. Heat flow

A list of classes A/B/C/D/G boreholes, calculated geothermal gradients, and heat flow determinations given for a total of 33 points are given in Table 2. Errors for gradients are calculated using the method of Chapra and Canale (2010). Generally, D class boreholes are disturbed

by IBF activity and are too shallow. Thus, the statistical distribution of geothermal gradients for classes A/B/C (total of 57 points) including the previously published data from Pfister et al., 1998 and Erkan, 2015 are shown in Figure 4a. Most of the geothermal gradient data lie between 30–50 °C km^{-1} and the mean conductive geothermal gradient is calculated as 37 ± 13 °C km^{-1} for the study area.

Thermal conductivity values were assigned according to the lithological information for the depths interval where the geothermal gradient is calculated. Available thermal conductivity measurements of surface outcrops were made on wet conditions. If thermal conductivity measurements were not available, literature values from Erkan (2015) and Balkan et al. (2017) were used.

The calculated heat flow values for the study area are listed in Table 2. The heat flow values of Intepe1 and Koprücek1 can not be calculated due to the lack of lithological information. The mean conductive heat flow is calculated to be 74 ± 22 mWm^{-2} based on A/B/C/ type data, and their statistical distribution is given in Figure 4b. The regional distribution of new heat flow data together with the previous heat flow data from Pfister et al. (1998) and Erkan (2015) is given in Figure 5. The elevated heat
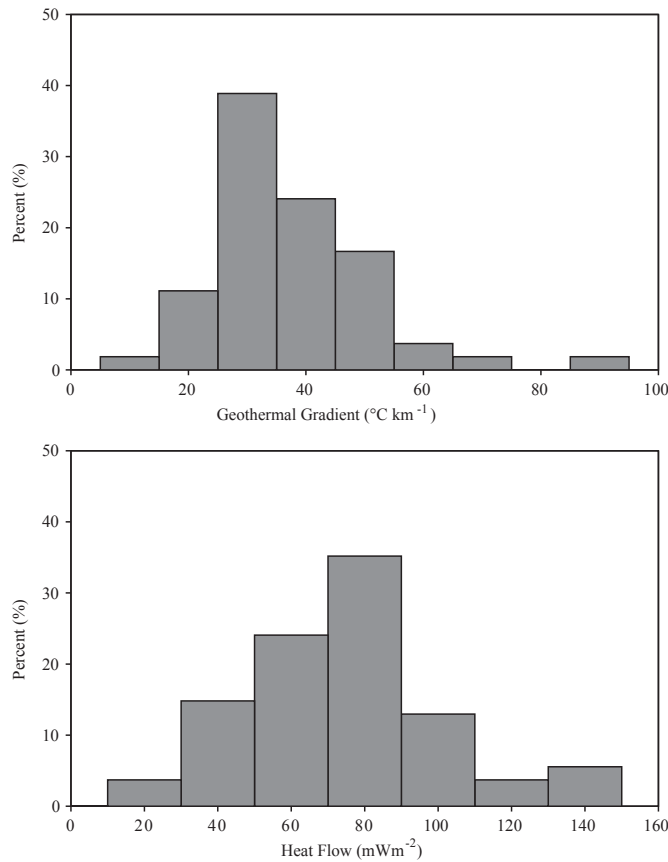
Figure 4. Histogram of the a) geothermal gradient, and b) heat flow using all class (A/B/C/ type) data.
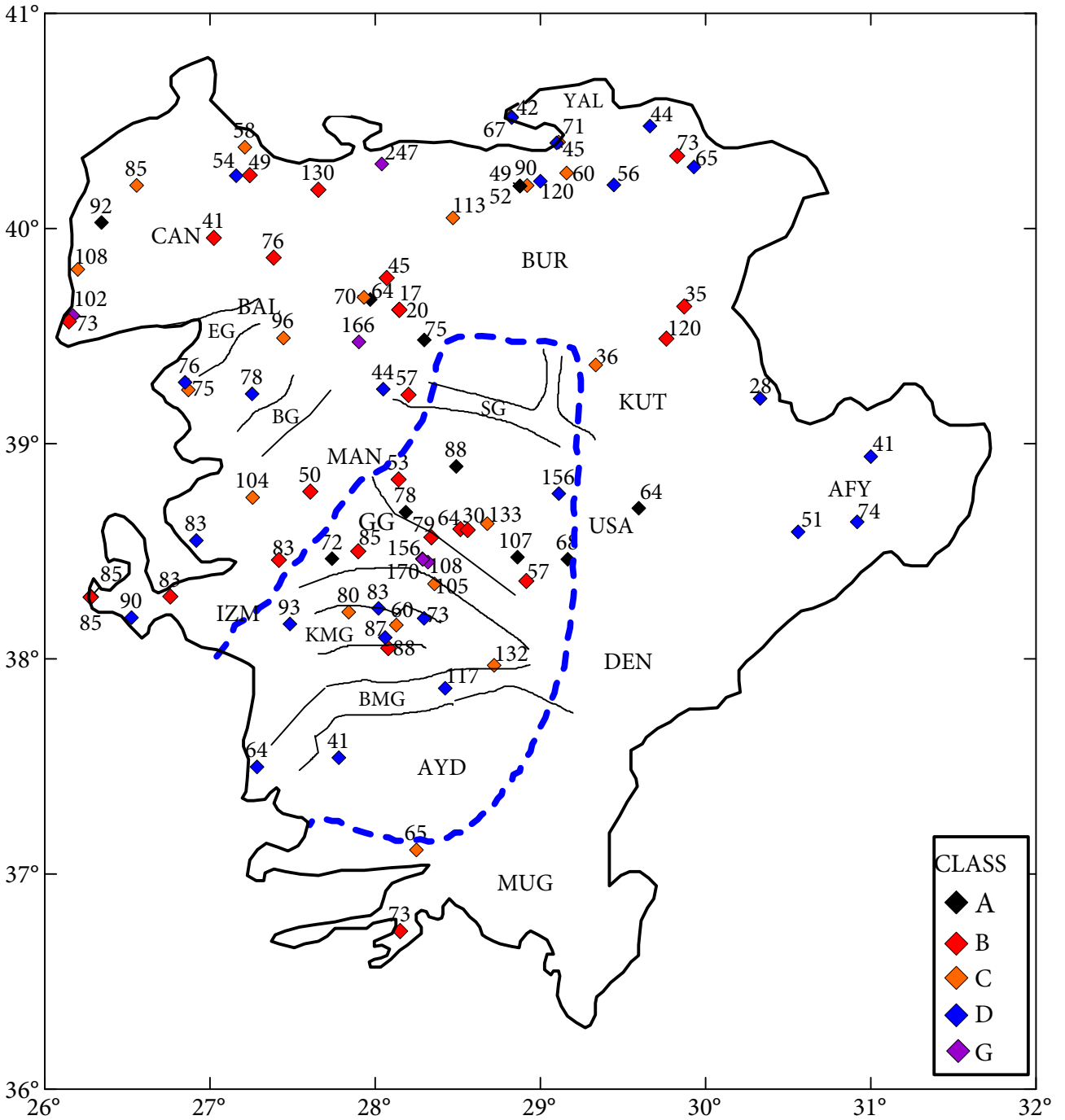
Figure 5. Regional distribution of new heat flow data together with the previous heat flow data from Pfister et al. (1998) and Erkan (2015). Black lines indicate boundaries of horst–graben structures. Blue dashed line indicates the border of Menderes Massif.

flow values are generally found within the basins located in Menderes Massif and the vicinity of hot springs. Göbekli (108 mWm^{-2}) Köseali (170 mWm^{-2}) and Köseali2 (156 mWm^{-2}) in Manisa are rated as G class they are located southern edge of Gediz graben. The northern part of the study (Balıkesir and Çanakkale) area is generally

characterized with moderate heat flow values with some exceptions. The middle-eastern part (Kütahya, Afyon, and Uşak) of the study area is represented with low-moderate values. Moderate to high heat flows are located in İzmir, around Ilıca hot spring in Çeşme peninsula and Küçük Menderes graben.

5.3. Correction of sedimentation and thermal refraction effect

Steady-state heat flow determinations in the extension-dominated regions may be perturbed by transient/long-term effects such as erosion/sedimentation and thermal refraction (Blackwell, 1983). The horst-graben systems located in the Menderes Massif form suitable conditions for the occurrence of these effects. Sedimentation in the grabens results in a reduction in the observed surface heat flow depending on the sedimentation rates. In opposite, the erosion process makes an increasing effect on the surface heat flow (Beardsmore and Cull, 2001). The thermal conductivity contrast between horst and graben fills causes thermal refraction at the boundary. Basin fills units with low thermal conductivity act as a thermal blanket refracting toward the horst. Thus, fluctuating heat flow values are observed at the boundaries of these structures (Thakur et al., 2012). Erkan (2015) applied a model for sedimentation/erosion effects based on using the module by Beardsmore and Cull (2001) for Menderes Massif. According to this, the surface heat flow decreases 10–15 mW m^{-2} with increasing sedimentation rates in the region. The erosion effect increases the surface heat flow up to 130 mW m^{-2} from a value of 85 mW m^{-2} without such an effect.

In the present data set, Bademli1, K.avulcuk, Pirlibey, and Osmancık points are located on the alluvial fans within the grabens. These points are expected to be under the effect of both sedimentation and thermal refraction. So, their values were corrected for sedimentation before being included in the heat flow contour map.

6. Discussion

The heat flow contour map of western Anatolia (Figure 6) is generated using only A/B/C class data given in Table 3 together with the previous results of Pfister et al. (1998) and Erkan (2015). The heat flow values outside the range of 40–140 mWm^{-2} are excluded due to the possible hydrologic disturbances. Erkan (2015) reported the preliminary heat flow data set for western Anatolia. In this study, we update it with the new heat flow data collected from Aydın, Balıkesir, Çanakkale, İzmir, Kütahya, and Manisa.

The western Anatolia region is presented by moderate to high heat flow values in the heat flow contour map (Figure 6). Generally, high values are observed around the Menderes Massif due to the intense tectonic activity. The highest heat flow values are recorded around the geological structures which are formed as a result of these activities. For example, heat flow at the intersection of E-W trending grabens within the Menderes massif is extremely high (Figure 6). Several exploration studies on Menderes Massif demonstrated its extremely high geothermal potential resulting in significant electric production (Serpen et al.,

2000; Roche at al., 2018). Contrary to general belief, the heat source of the region is not of magmatic origin in the region. Recent studies suggested that regional thermal anomalies are associated with active extension tectonics related to the Aegean slab dynamics driven by the retreat of the subduction of the African lithosphere beneath the Hellenic and Cyprus trenches (Roche et al., 2018). Locally higher heat flow values around the Alaşehir part of the Gediz graben in accordance with existing geothermal areas and shallow Curie point depth (Dolmaz et al., 2005; Bilim et al., 2016). The area around the Kula, the unique volcano arisen from recent volcanic activity, is presented by high values. This anomaly is also mentioned in previous studies (Tezcan and Turgay, 1991; Erkan, 2015). On the other hand, the northeastern part of Çanakkale and central of Balıkesir and Yalova regions are characterized with moderate heat flow values. In the central part of Balıkesir and the eastern part of Çanakkale, local hydrological effects are considered to be responsible for relatively low heat flow values. The coastal site of Çanakkale is denoted with higher heat flow values and host many hot springs associated with geothermal systems, whereas it is opposite in the central part. Therefore, temperature measurements in deep boreholes are suggested for detailed interpretations for the Çanakkale region.

Seismological studies describe the study region with lower velocities than average continental values (Akyol et al., 2006) emphasizing high heat flow values. Interpretation of heat flow distribution with b-values in a region reveals the deep structural features. b-values are associated with directly tectonic and thermal characteristics and high b-values correspond to high thermal gradients (Warren & Latham, 1970; Katsumata, 2006; Kalyoncuoğlu et al., 2013). Sayil & Osmanşahin (2008) and Bayrak & Bayrak (2012) reported b-values for the sub-regions of western Anatolia in their studies. The highest b-values are obtained around the Gediz graben in both studies, which are in coincidence with high heat flow values in this study.

6. 1. Thermal model of Gediz graben

Heat flow determinations show that heat flow is distinctively high in Alaşehir part of Gediz graben. Many geophysical and geological studies emphasize the importance of Gediz graben by means of the geothermal perspective. However, no thermo-mechanical model has been presented up to date. Modeling studies are crucial where it is not possible to measure temperature within the deeper parts of Earth. Calculation of the geothermal heat available at a certain depth requires subsurface temperature distribution among the other parameters. We present, for the first time, temperature distribution within the graben that helps to examine the geothermal potential of Gediz graben as a sedimentary basin.
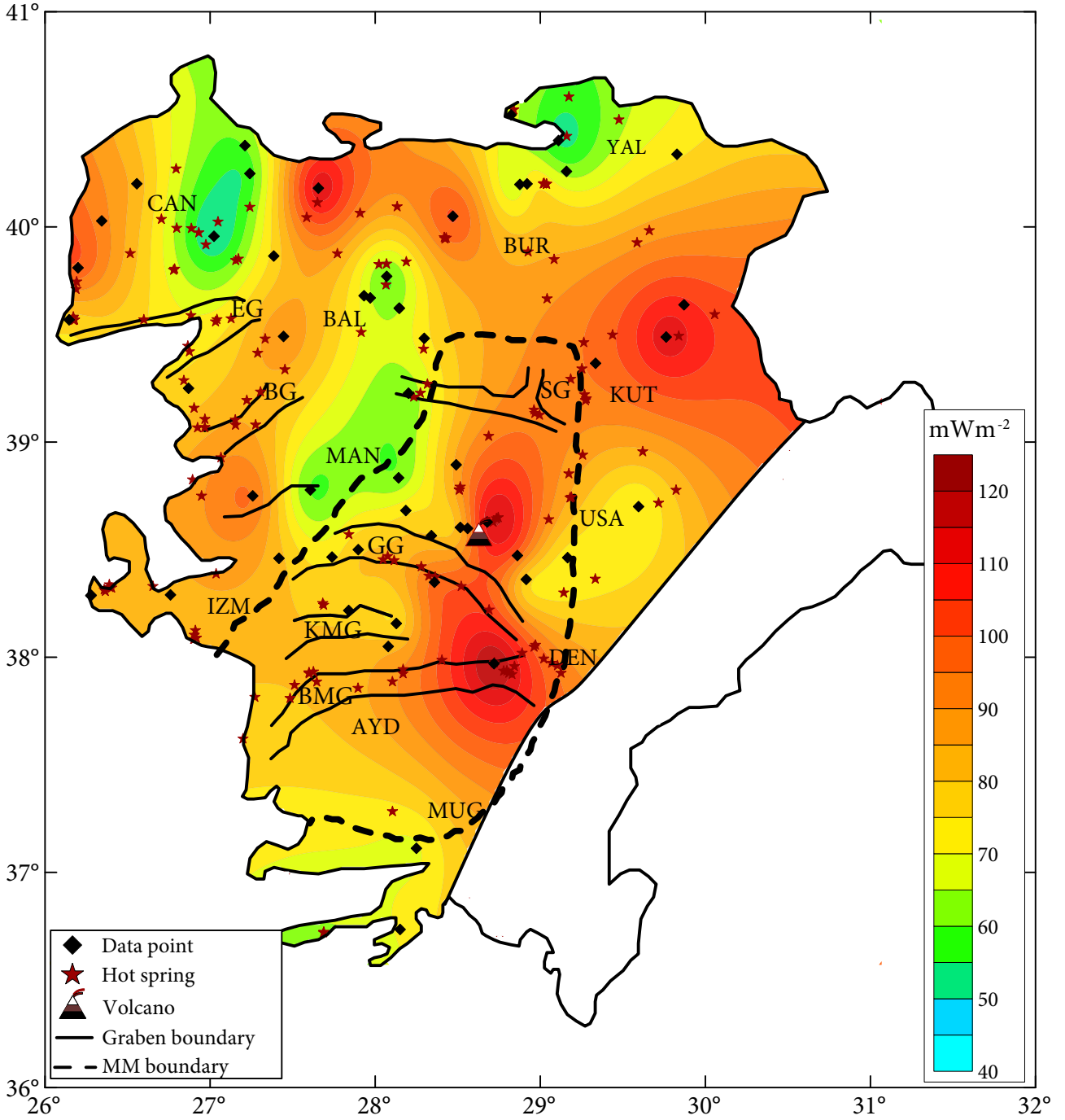
Figure. 6. The heat flow map of western Anatolia using the results of this study with those of Erkan (2015) and Pfister et al. (1998). Red star symbols show locations of hot springs. Black lines indicate boundaries of horst–graben structures, GG: Gediz Graben; BMG: Büyük Menderes Graben; KMG: Küçük Menderes Graben; EG: Edremit Graben; BG: Bakırçay Graben; SG: Simav Graben.

2D steady-state heat conduction differential equation is solved, under the conductive heat transfer assumption, to obtain temperature distribution within the graben. Finite elements methods-based numerical modeling software Comsol Multiphysics is implemented to obtain forward modeling results.

The model geometry of the graben is generated using previously published geological cross-sections based on the seismic reflection data (Figure 2a) (Çiftçi and Bozkurt, 2009a; Çiftçi et al., 2010). The model consists of a single basement unit and sedimentary fill, which is divided into four sub-sections based on thermal conductivity

Table 3. Thermal property values used in the Gediz Graben model.

Dominant Lithology	Seismic Stratigraphic Unit	Thermal Conductivity λ(W/ m K)	Heat production A(μW/m³)
Loose conglomerate-clastic rocks	Quaternary alluvium	1.50[a]	1.12[c]
Conglomerate-Sandstone-Mudstone	SSU-III	2.56	1.12[c]
Sandstone-Mudstone-Conglomerate-Limestone	SSU-II	2.67	1.12[c]
Shale-Conglomerate-Sandstone-Mudstone	SSU-I	2.45	1.12[c]
Schist-Marble-Quartzite	Basement	3.10[b]	1.88[c]

Parameter values are derived from [a]Erkan (2015), [b]Balkan et al. (2017), [c]Şahin (2014).

properties. Dirichlet boundary condition is fixed at 18 °C on the surface of the model, which is the annual mean temperature for the region (Şensoy et al., 2008), while a constant Neumann boundary condition is set at the bottom of the model (6 km depth). It is assumed that the sides of the model are thermally insulated implying no lateral heat flow at the sides of the model.

Radiogenic heat production values in the basement and sedimentary rocks are included in the model. The knowledge of heat production distribution of the common rock types of the model is obtained from data compiled by Şahin (2014). The measured thermal conductivity values are applied as a constant value for each stratigraphic unit, whereas Quaternary alluvium and basement units are assigned from the literature as given in Table 3. The temperature dependence of thermal conductivity is taken into account using the equation developed by Kukkonen and Jöeleht (1996) and ignored the minor effect of pressure on thermal conductivity. The goal of the model is to obtain the best match between calculated and measured temperatures for deep boreholes (BH-1 and BH-2) by varying the heat flow at the bottom of the model.

For the final model, a very good agreement between measured and calculated temperatures is observed, while constant heat flow at the bottom of the model equals to 78 mW m^{-2}. The root mean square error (rms) runs to 2.06 °C for BH-1 and 2.8 °C for BH-2 (corresponding to an rms of 2.4%, n = 9 and 1.5 %, n = 22 respectively) (Figure 7a and Figure 7b). Calculated heat flow profile at the surface of Gediz graben ranges between 77–150 mWm^{-2} (Figure 8a). Surface heat flow appears to increase symmetrically at the contact of the basement and sedimentary rock due to the thermal conductivity contras between them. This anomalously increase can be explained by heat refraction. The heat coming from the bottom of the graben transfers through the basement rocks with high thermal conductivity causes to high temperature at the edge of the sedimentary fill. Due to the low thermal conductivity of graben fill rocks, heat cannot transfer into the basin (Beardsmore 2004; Thakur et al., 2012). Calculated surface

heat flows values are in accordance with the measured values in Gediz graben (Figure 6 and Table 2).

The predicted temperature distribution within the basin is given in Figure 8b. The higher temperatures are calculated in sub-basinal areas where the thermal conductivity contrast between basin fill and basement rock is more significant. The basins with thicker sedimentary fills have their isotherms bent upward and thus referring to higher geothermal gradients. The thickness of the basin fill reaches 3000 m meters in the middle of the model where the temperature of 140 °C is calculated and the maximum temperature reaches 243 °C at the bottom of the model (Figure 8b). Some mismatches, between modeling results and measurements (Figure 7) may be attributed to additional heat transport by groundwater flow in the subsurface which is not taken into account in the present model. The hydro-geological effect, heterogeneities in the sedimentary sequences within the graben, and local groundwater flow existed from the fault zone may disturb the temperature-depth curves.

The modeling results and the comparisons with the available measurements provide us some quantitative measures of the surface heat flow in Gediz graben. Considering the minority of the mismatch between the model and measured temperatures, we conclude that the temperatures are mainly controlled by thermal conduction within the graben. These results can be used to derive the geothermal energy potential of the study area. Depths with temperatures of greater than 150–200 °C can be the target level for future EGS studies.

7. Conclusion
This study reports the updated heat flow map of western Anatolia with 33 new heat flow data. The new heat flow map has higher data density in some areas; in particular, in Menderes Massif, there is greater variability in heat flow than previous maps (Tezcan and Turgay, 1991; Erkan, 2015). The new heat flow data have added to our knowledge of geologic regions, particularly in Menderes Massif. The maximum heat value is evaluated in the intersection point
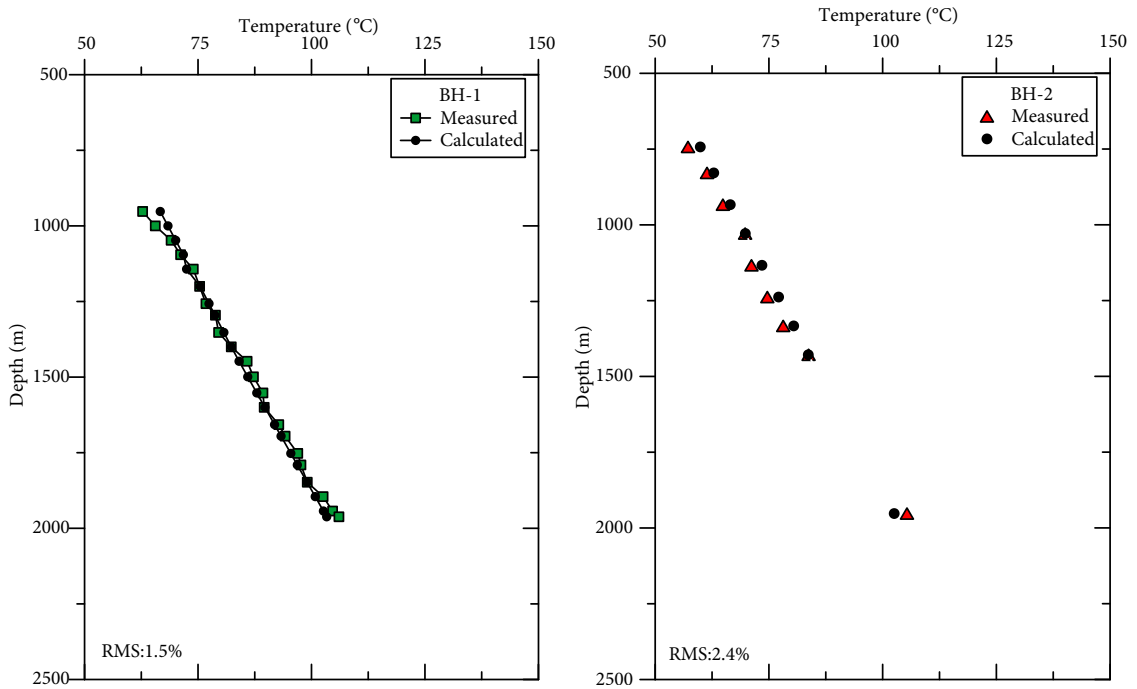
Figure 7. Comparison between modeled and observed borehole temperatures for a) BH-1 and, b) BH-2.
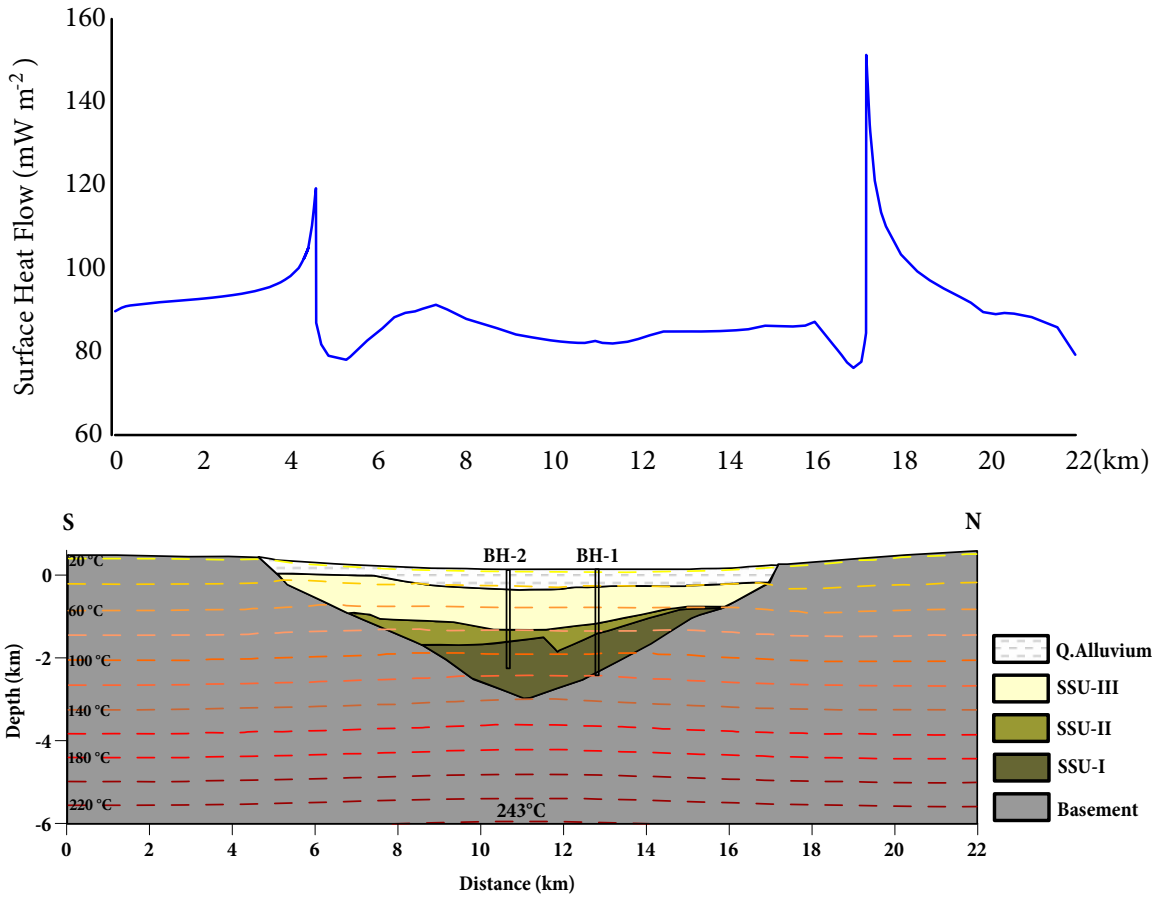
Figure 8. The calculated a) surface heat flow, and b) 2D subsurface temperature distribution.

of the Büyük Menderes and Gediz grabens. The existing greater number of data in Gediz graben allows us to examine its thermal structure in detail. Thus, 2D numerical temperature models have been developed for Gediz graben. The forward modeling approach is novel as it is performed for the first time a comprehensive investigation of high precision T-D data. Our results show that relatively high heat flow values around Gediz graben may be explained by 2D steady-state conductive thermal modeling. According to the results, the temperature distribution within the graben is mainly controlled by sedimentary fill with low thermal conductivity. The insulating effects of the entire sediment fill result in a long-wavelength variation of temperatures in response to heat refraction effects caused by the contrast between insulating sedimentary rocks and

highly conductive basement metamorphic. We concluded the maximum temperature at the base of the sedimentary fills and the basement reaches 140 °C and 243 °C, respectively in Gediz graben. These temperatures greater than 150°C, required for EGS, can be found at a reasonable depth of < 5 km.

References

Baba A (2012). Present energy status and geothermal utilization in Turkey. In: 39th International Association of Hydrogeologists; Canada. pp. 16-21.

Balkan E, Erkan K, Şalk M (2017). Thermal conductivity of major rock types in western and central Anatolia regions, Turkey. Journal of Geophysics and Engineering 14 (4): 909-919. doi: 10.1088/1742-2140/aa5831

Beardsmore GR (2004). The influence of basement on surface heat flow in the Cooper Basin. Exploration Geophysics 35 (4): 223–35. doi: 10.1071/EG04223

Beardsmore GR, Cull JP (2001). Crustal heat flow: a guide to measurement and modelling. Cambridge University Press.

Bellani S, Gherardi F (2019). Thermal conductivity characterization of Larderello and Mt. Amiata geothermal fields, Italy. GRC Transactions 43: 541-549.

Bilim F, Akay T, Aydemir A, Kosaroglu S (2016). Curie point depth, heat-flow and radiogenic heat production deduced from the spectral analysis of the aeromagnetic data for geothermal investigation on the Menderes Massif and the Aegean Region, western Turkey. Geothermics 60: 44–57. doi: 10.1016/j.geothermics.2015.12.002

Blackwell DD (1983). Heat flow in the northern Basin and Range province. Geothermal Resources Council Special Report 13: 81-92.

Bozkurt E (2001). Neotectonics of Turkey—a synthesis. Geodinamica Acta 14: 3–30. doi: 10.1080/09853111.2001.11432432

Burçak M (2012). Kizgin Kuru Kaya (HDR: Hot Dry Rock) Ve Geliştirilebilir Jeotermal Sistemler (EGS: Enhanced Geothermal Systems). Maden Tetkik ve Arama Genel Müdürlüğü, Enerji Hammadde Etüt ve Arama Dairesi. Ankara (in Turkish).

Burçak M (2015). Hot dry rock (HDR) and enhanced geothermal system (EGS) and favourable regions for innovation in Turkey. MTA 80. Yıl Sempozyumu, Ankara (in Turkish).

Cermak V, Rybach L (1979). Terrestrial heat flow in Europe. Berlin: Springer Verlag.

Chapra SC, Canale RP (2011). Numerical methods for engineers (Vol. 2). New York: Mcgraw-hill.

Çağlar KÖ (1961). Türkiye maden suları ve kaplıcaları. Seri B (no:11). Ankara, Maden Tetkik ve Arama Enstitüsü Yayınları (in Turkish).

Çanakci H, Demirboğa R, Karakoç MB, Şirin O (2007). Thermal conductivity of limestone from Gaziantep (Turkey). Building and Environment 42 (44): 1777-1782. doi: 10.1016/j.buildenv.2006.01.011

Çiftçi N B, Bozkurt E (2009a). Evolution of the Miocene sedimentary fill of the Gediz Graben, SW Turkey. Sedimentary Geology 216 (3): 49-79. doi: 10.1016/j.sedgeo.2009.01.004

Çiftçi NB, Bozkurt E (2009b). Pattern of normal faulting in the Gediz Graben, SW Turkey. Tectonophysics 473 (1): 234-260.

Çiftçi NB, Bozkurt E (2010). Structural evolution of the Gediz Graben, SW Turkey: temporal and spatial variation of the graben basin. Basin Research 22 (6): 846-873.

Çiftçi NB, Temel RO, İztan YH (2010). Hydrocarbon occurrences in the western Anatolian (Aegean) grabens, Turkey: Is there a working petroleum system?. American Association of Petroleum Geologists Bulletin 94 (12): 1827-1857. doi: 10.1306/06301009172

Demirboğa R (2003). Influence of mineral admixtures on thermal conductivity and compressive strength of mortar. Energy and Buildings 35 (2): 189-192. doi: 10.1016/S0378-7788(02)00052-X

Demirel Z, Sentürk N (1996). Geology and hydrogeology of deep thermal aquifers in Turkey. In: Proceeding of the Regional Seminar on Integration of Information Between Oil Drilling and Hydrogeology of Deep Aquifers. Amman, Jordan. pp. 38.

Dewey JF, Şengör AMC (1979). Aegean and surrounding regions: complex multiple and continuum tectonics in a convergent zone. Geological Society of America Bulletin 90 (1): 84–92.

Dolmaz MN, Ustaömer T, Hisarli ZM, Orbay N (2005) Curie point depth variations to infer thermal structure of the crust at the African-Eurasian convergence zone, SW Turkey. Earth Planets and Space 57 (5): 373–38.

Emre T (1996). Geology and tectonics of the Gediz graben. Turkish Journal of Earth Science 5 (3): 171–185.

Erkan K (2015). Geothermal investigations in western Anatolia using equilibrium temperatures from shallow boreholes. Solid Earth 6 (1): 103-113. doi: 10.5194/se-6-103-2015

Grubbe K, Haenel R, Zoth G (1983). Determination of the vertical component of thermal conductivity by line source methods. Zentralbl Geol. Palaontol. 1: 49–56.

Gülmez F, Damcı E, Ülgen UB, Okay A (2019). Deep Structure of Central Menderes Massif: data from deep geothermal wells. Turkish Journal of Earth Sciences 28: 531-543.

Gürer A, Pinçe A, Gürer Ö F, İlkışık O M (2002). Resistivity distribution in the Gediz Graben and its implications for crustal structure. Turkish Journal of Earth Sciences 11 (1): 15-25.

Hakyemez HY, Erkal T, Göktas F (1999). Late Quaternary evolution of the Gediz and Büyük menderes grabens, western Anatolia, Turkey. Quaternary Science Reviews 18 (4-5): 549-554. doi: 10.1016/S0277-3791(98)00096-1

Healy JJ, de Groot JJ, Kestin J (1976). The theory of the transient hot-wire method for measuring thermal conductivity. Physica B+C 82 (2): 392-408. doi: 10.1016/0378-4363(76)90203-5.

Hıdıroğlu İA, Parlaktuna M (2019). Dünyada Kızgın Kuru Kaya (HDR) Projeleri ve Türkiye'nin Muhtemel HDR Alanları. Jeotermal Elektrik Santral Yatırımcıları Derneği, 6-7 Şubat GT2019 Türkiye Jeotermal Kongresi Bildiriler Kitabı Ankara. Turkey. pp. 91-103.

Işık V, Tekeli O (2001). Late orogenic crustal extension in the northern Menderes Massif (Western Turkey); evidence for metamorphic core complex formation. International Journal of Earth Science 89: 757-765.

İlkışık OM, Yalçın MN, Sari C, Okay N, Bayrak M et al. (1996a). Ege bölgesi'nde ısı akısı araştırmaları, TÜBİTAK Proje No: YDABÇAG-233/G, Ankara (in Turkish).

İlkışık OM., Sarı C, Bayrak M, Öztürk S, Sener Ç et al. (1996b). Ege bölgesinde jeotermik araştırmalar, TÜBİTAK, Proje No: YDABÇAG-430/G, Ankara (in Turkish).

Jaeger JC (1965). Application of the theory of heat conduction to geothermal measurements. In: Lee WHK (editor).Terrestrial Heat Flow. Washington:American Geophysical Union. pp. 7-23.

Jaupart C, Labrosse S (2007). Temperatures, heat and energy in the mantle of the earth. Treatise on Geophysics 7: 223-270.

Karakuş H (2013). Geothermal energy in active extensional basins: An example from Western Anatolia, Turkey. In: (Jianwen Yang) Geothermal Energy, Technology and Geology. Newyork; Nova, pp. 115-150.

Karakuş H, Şimşek Ş (2012). Spatial variations of carbon and Helium isotope rations in geothermal fluids of Buyuk Menderes Graben. In: 5th Geochemistry Symposium. pp. 23-25.

Kukkonen IT, Jõeleht A (1996). Geothermal modelling of the lithosphere in the central Baltic Shield and its southern slope. Tectonophysics 255 (1): 25-45.

Lee WH, Uyeda S (editors) (1965). Review of heat flow data: Terrestrial heat flow. Washington, American Geophysical Union.

Lees CH (1910). On the shapes of the isogeotherms under mountain ranges in radio-active districts. Proceedings of the Royal Society of London. Series A, Containing Papers of a Mathematical and Physical Character 83 (563): 339-346.

Le Pichon X, Chamot-Rooke N, Lallemant S, Noomen R, Veis G (1995). Geodetic determination of the kinematics of central Greece with respect to Europe: Implications for eastern Mediterranean tectonics. Journal of Geophysical Research: Solid Earth 100(B7): 12675-12690. doi: 10.1029/95JB00317

Lowrie W (2007). Fundamentals of geophysics (2nd ed.). Newyork: Cambridge University Press.

Özyalın Ş, Pamukçu O, Gönenç T, Yurdakul A, Sözbilir H (2012). Application of boundary analysis and modeling methods on Bouguer gravity data of the Gediz Graben and surrounding area in Western Anatolia and its tectonic implications. Journal of the Balkan Geophysical Society 15 (2): 19-30.

Paton S (1992). Active normal faulting, drainage patterns and sedimentation in southwestern Turkey. Journal of the Geological Society 149 (6): 1031-1044. doi: 10.1144/gsjgs.149.6.1031

Pollack HN, Chapman D S (1977). On the regional variation of heat flow, geotherms, and lithospheric thickness. Tectonophysics 38 (3-4): 279-296. doi: 10.1016/0040-1951(77)90215-3

Pfister M, Ryback L, Şimşek Ş (1998). Geothermal reconnaissance of the Marmara Sea region (NW Turkey): surface heat flow density in an area of active continental extension. Tectonophysics 291 (1-4): 77–89. doi: 10.1016/S0040-1951(98)00032-8

Roche V, Sternai P, Guillou-Frottier L, Menant A, Jolivet L et al. (2018) Emplacement of metamorphic core complexes and associated geothermal systems controlled by slab dynamics. Earth and Planetary Scince Letters 498 (15): 322–33. doi: 10.1016/j.epsl.2018.06.043

Roche V, Bouchot V, Beccaletto L, Jolivet L, Guillou-Frottier L et al. (2019). Structural, lithological, and geodynamic controls on geothermal activity in the Menderes geothermal Province (Western Anatolia, Turkey). International Journal of Earth Sciences 108 (1): 301–328. doi: 10.1007/s00531-018-1655-1

Sarı C, Şalk M (2006). Sediment thicknesses of the western Anatolia graben structures determined by 2D and 3D analysis using gravity data. Journal of Asian Earth Sciences 26 (1): 39-48. doi: 10.1016/j.jseaes.2004.09.011

Sass JH, Lachenbruch AH, Moses TH, Morgan P (1992). Heat flow from a scientific research well at Cajon Pass, California. Journal of Geophysical Research: Solid Earth, 97 (B4): 5017-5030. doi: 10.1029/91JB01504

Sözbilir H (2002). Geometry and origin of folding in the Neogene sediments of the Gediz Graben, western Anatolia, Turkey. Geodinamica Acta 15: 277–288. doi: 10.1080/09853111.2002.10510761

Şahin S (2014). Gediz grabeni Alaşehir bölgesinin jeotermal potansiyelinin jeofizik yöntemlerle araştırılması. MSc Thesis, Çanakkale Onsekiz Mart University, Çanakkale, Turkey (in Turkish).

Şengör AMC, Görür N, Şaroçlu F (1985). Strike-slip faulting and related basin formations in zones of tectonic escape: Turkey as a Case Study. In: Biddle KT, Christie-Blick N (editors) Strike-slip Faulting and Basin Formation. Soc. Econ. Paleontol. Mineral. Special Publication, pp. 227–264

Şensoy S, Demircan M, Ulupınar U, Balta İ (2008). Türkiye iklim atlası. Turkish State Meteorological Service (DMİ), Ankara. (in Turhish).

Tezcan AK, Turgay MI (1991). Heat flow and temperature distribution in Turkey. Geothermal atlas of Europe. Gotha: Herman Haack Verlag.

Thakur M, Blackwell DD, Erkan K (2012). The Regional thermal regime in Dixie Valley, Nevada, USA. Geothermal Resources Council Transactions 36: 59-67.

Thienprasert A, Raksaskulwong M (1984). Heat flow in northern Thailand. Tectonophysics 103 (1-4): 217-233. doi: 10.1016/0040-1951(84)90085-4

Yılmaz Y, Genç ŞC, Gürer F, Bozcu M, Yılmaz K et al. (2000). When did the Western Anatolian grabens begin to develop? In: Bozkurt E, Winchester, JA, Piper JAD (editors). Tectonics and Magmatism in Turkey and the Surrounding Area. Journal of Geological Society of London special Publication. pp. 131–162.